Electrostatic Assemblies of Fullerene−Porphyrin Hybrids: Toward Long-Lived Charge Separation

Domenico Balbinot,[†] Stefan Atalick,[‡] Dirk M. Guldi,*[,‡] Maria Hatzimarinaki,[†] Andreas Hirsch,*[,†] and Norbert Jux*[,†]

Institut für Organische Chemie der Universität Erlangen-Nürnberg, Henkestrasse 42, D-91054 Erlangen, Germany, and Radiation Laboratory, University of Notre Dame, Notre Dame, Indiana 46556

Received: April 18, 2003; In Final Form: September 22, 2003

The Coulomb complex formation of a dendritic fullerene oligocarboxylate ($\mathbf{1}^{8-}$) and an octapyridinium zinc porphyrin salt ($\mathbf{ZnP}^{8+}$) was investigated. A Job plot obtained by monitoring the Soret absorption of $\mathbf{ZnP}^{8+}$ upon addition of **1** in a phosphate buffer (pH 7.2, ionic strength = 0.012) indicated the formation of a 1:1 complex, $\mathbf{ZnP}^{8+}/\mathbf{1}^{8-}$, for which an association constant of $(3.5 \pm 1.0) \times 10^8$ M^{-1} was determined. Parallel fluorescence titration experiments revealed that the $\mathbf{ZnP}^{8+}$ emission is strongly quenched in the $\mathbf{ZnP}^{8+}/\mathbf{1}^{8-}$ complex. In particular, the noted decrease of fluorescence intensity in $\mathbf{ZnP}^{8+}$ with variation of $\mathbf{1}^{8-}$ and evidence for a new short-lived emissive component suggest a static quenching event inside a $\mathbf{ZnP}^{8+}/\mathbf{1}^{8-}$ complex. From the fluorescence titration, a value of $(1.1 \pm 0.1) \times 10^8$ M^{-1} for the association constant of the $\mathbf{ZnP}^{8+}/\mathbf{1}^{8-}$ complex at pH 7.2 was derived. The association constant decreased, however, when the ionic strength of the solution was raised. Electron-transfer quenching was confirmed by transient absorption spectroscopy, which showed the fingerprint absorptions of the $\mathbf{ZnP}^{8+}$ radical cation and the $\mathbf{1}^{8-}$ radical anion and a lifetime of 1.1 μs for the charge-separated state. Molecular dynamic simulations offer insight into the supramolecular structure of the fullerene−porphyrin hybrid, $\mathbf{ZnP}^{8+}/\mathbf{1}^{8-}$.

Introduction

Coulomb interactions are of fundamental importance in nature and are employed in several facets in biological systems. They provide, for example, the electrostatic environment of proteins, which, in turn, governs their binding affinities and reactivities. It comes as no surprise that the interactions of charged molecules with biomolecules have been studied extensively. Hybridization of proteins with molecules that modify their function in terms of electron transfer[1] and conformational[2] behavior is currently an important topic within bioorganic chemistry. Such aggregation phenomena and their concomitant electron transfer events are of elemental interest not only because of their obvious importance in nature but also as guiding principles in materials sciences.[3]

We discovered recently that the monoadduct fullerene dendrimer system **1** (Scheme 1) in its 8-fold deprotonated state efficiently hybridizes with mitochondrial cytochrome *c* (**Cyt*c***), a polycationic redox protein. In contrast to other fullerene systems, in particular fullerene hexaadducts,[4] the characteristic electron acceptor behavior of parent $\mathbf{C_{60}}$ is mostly preserved in **1**. Also, **1** is soluble in phosphate-buffered aqueous solutions (pH 7.2), in which the octaanion $\mathbf{1}^{8-}$ is the predominant species, allowing for complexation studies with **Cyt*c*** under homogeneous conditions. We found that $\mathbf{1}^{8-}$ strongly binds to **ZnCyt*c*** with an association constant of $(3.1 \pm 0.4) \times 10^5$ M^{-1} at pH 7.2. A photoinduced electron transfer led to the formation of a charge-separated species with a lifetime of 1.8 μs.[5]

On the basis of these findings, we introduce here the first example of a general modular concept for the electrostatically driven hybridization of nonnatural—and more easily investigated—oligoelectrolytes including their electronic communication. The corresponding modules should exhibit well-defined structural properties and carry sufficient charges to guarantee strong binding (Figure 1). This approach gives access to *discrete* functional supramolecular assemblies,[6] which can act not only as biomimetic model systems for natural peptide hybridization but also as redox-active, pH-switchable novel materials. Related to this approach are contributions by Fuhrhop et al., who investigated the dimerization and trimerization of various ionic porphyrin derivatives.[7] Contrasting with our approach is Fuhrhop's use of chromophores of similar type and shape. We chose the abovementioned anionic dendritic fullerene **1**, as well as a cationic porphyrin, $\mathbf{ZnP}^{8+}$, as a set of oppositely charged and water-soluble modules because of their well-defined architectures and their compatibility in size and charges (Scheme 1).[8] Furthermore, it seemed appropriate with regard to our modular concept to choose a porphyrin as counterpart of **1** because porphyrins provide unique electronic,[9] chemical,[10] and biological[11] properties. $\mathbf{ZnP}^{8+}$ carries the charges, contrasting to other cationic porphyrins, not within but above or below the porphyrin plane or both.[12] The globular shape of $\mathbf{ZnP}^{8+}$ is fairly rigid but can easily adapt to changes in the environment, which makes $\mathbf{ZnP}^{8+}$ an ideal model for **Cyt*c***.

The combination of the two modules, $\mathbf{1}^{8-}$ and $\mathbf{ZnP}^{8+}$, leads to the stable supramolecular assembly $\mathbf{ZnP}^{8+}/\mathbf{1}^{8-}$, which gives rise to a photoinduced intracomplex electron transfer.

* To whom correspondence should be addressed. E-mail addresses: Guldi.1@nd.edu; Hirsch@organik.uni-erlangen.de; jux@organik.uni-erlangen.de.

[†] Universität Erlangen-Nürnberg.

[‡] University of Notre Dame.

10.1021/jp0304780 CCC: $25.00 © 2003 American Chemical Society
Published on Web 11/08/2003

SCHEME 1: Dendrimer Fullerene Polyelectrolyte 1 and Octakis(pyridinium) Zinc Porphyrin ZnP^{8+} (CPK Models based on PM3 Calculations)

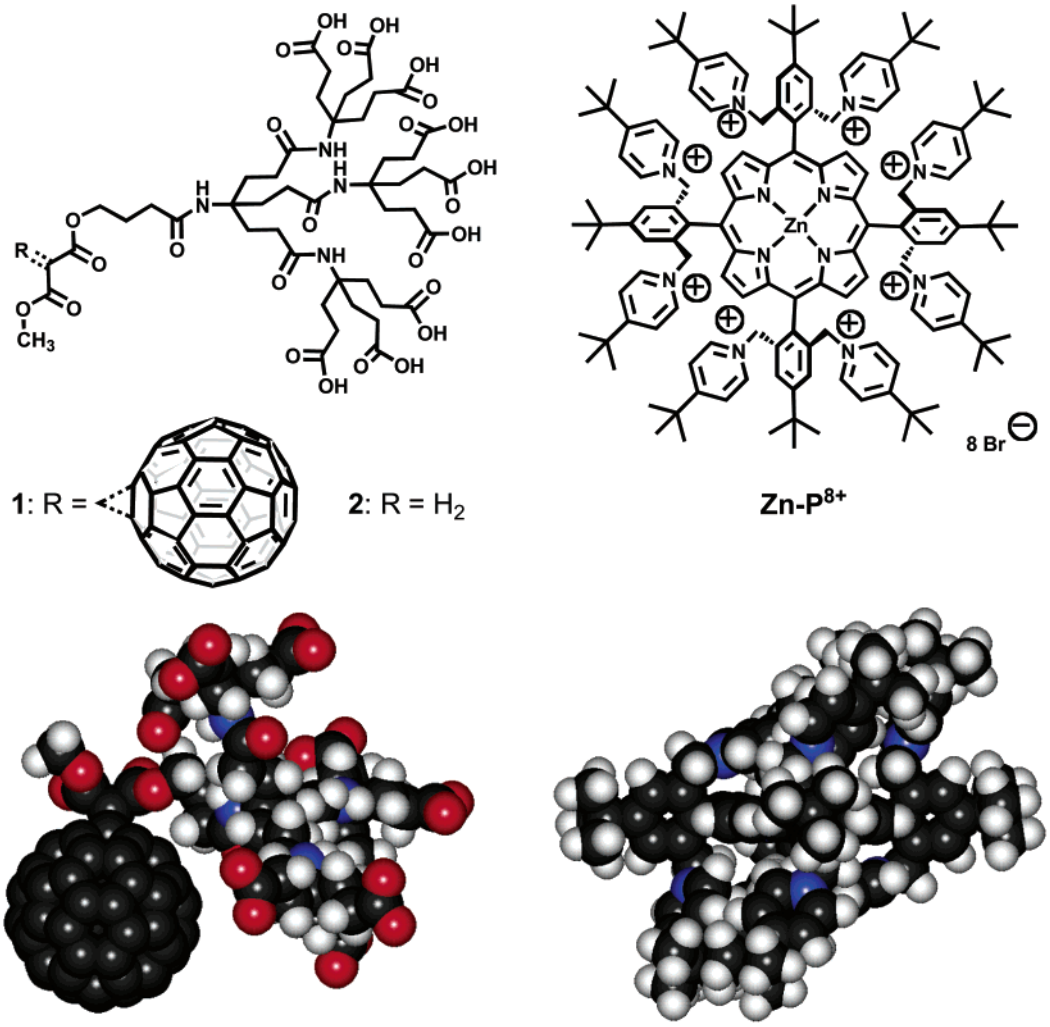

Experimental Methods

Stock solutions of $\mathbf{ZnP^{8+}}$ ($c_{por} = 3.58 \times 10^{-5}$ M) and $\mathbf{1^{8-}}$ ($c_{ful} = 3.89 \times 10^{-5}$ M) in phosphate-buffered solutions of pH 7.2 (ionic strength = 0.012) were prepared. Over a concentration range of 0.1×10^{-6} to 5×10^{-5} M, solutions of both $\mathbf{ZnP^{8+}}$- and $\mathbf{1^{8-}}$ follow the Lambert−Beer law. According to the method of continuous variation of the concentration with constant total concentration (Job's plot), 25 mixtures with a total concentration of $c_{tot} = 3.50 \times 10^{-6}$ M were prepared. The changes of the absorption of the Soret band of $\mathbf{ZnP^{8+}}$ were monitored. The expected absorption was subtracted from the experimental absorption and the resulting "corrected" absorption was plotted versus the mole fraction of $\mathbf{1^{8-}}$.[13] Figure 1 was obtained by generating a fourth-power fit on the whole data set, which gives a maximum at a molar fraction of $\mathbf{1^{8-}}$ of 0.52 with an absorption of 0.1840. The data points starting from molar fractions of $\mathbf{1^{8-}}$ = 0.0−0.5 and those from 0.5 to 1.0 were subjected to a linear fit each. The cross point of both lines was calculated to be at 0.52/0.2075. The corrected absorption values of the whole data set were then normalized by division with 0.2075, which leads the maximum of the fourth-power curve to a value of 0.88. According to Likussar,[13] this leads with the total concentration of the solutions of 3.5×10^{-6} M to an association constant of $(3.5 \pm 1.0) \times 10^{8}$ M^{-1}. Because of the low concentrations of $\mathbf{ZnP^{8+}}$and $\mathbf{1^{8-}}$, the margins of error for the absorptions are rather large, ranging in the order of approximately 15%. Changes of the ionic strength during the complexation studies were considered to be negligible because of the low concentrations of the components. The absorption spectra were recorded on a Shimadzu UV-3102 PC UV/vis-NIR scanning spectrophotometer.

Fluorescence lifetimes were measured with a laser strobe fluorescence lifetime spectrometer (Photon Technology International) with 337 nm laser pulses from a nitrogen laser fiber-coupled to a lens-based T-format sample compartment equipped with a stroboscopic detector. Details of the stroboscopic laser/detector systems are described on the manufacture's web site, http://www.pti-nj.com. Emission spectra were recorded with a SLM 8100 spectrofluorometer. The experiments were performed at room temperature. Each spectrum represents an average of at least five individual scans, and appropriate corrections were applied whenever necessary. Nano- to millisecond laser flash photolysis experiments were performed with laser pulses from a Quanta-Ray CDR Nd:YAG system (532 nm, 6 ns pulse width) in a front face excitation geometry. A Xe lamp was triggered synchronously with the laser. A monochromator (SPEX) in combination with either a Hamamatsu R 5108 photomultiplier or a fast InGaAs diode was employed to monitor transient absorption spectra.

All calculations were performed with the program package HyperChem.[14] The dendritic fullerene anion $\mathbf{1^{8-}}$ and the octacationic $\mathbf{ZnP^{8+}}$ were semiempirically optimized (PM3).

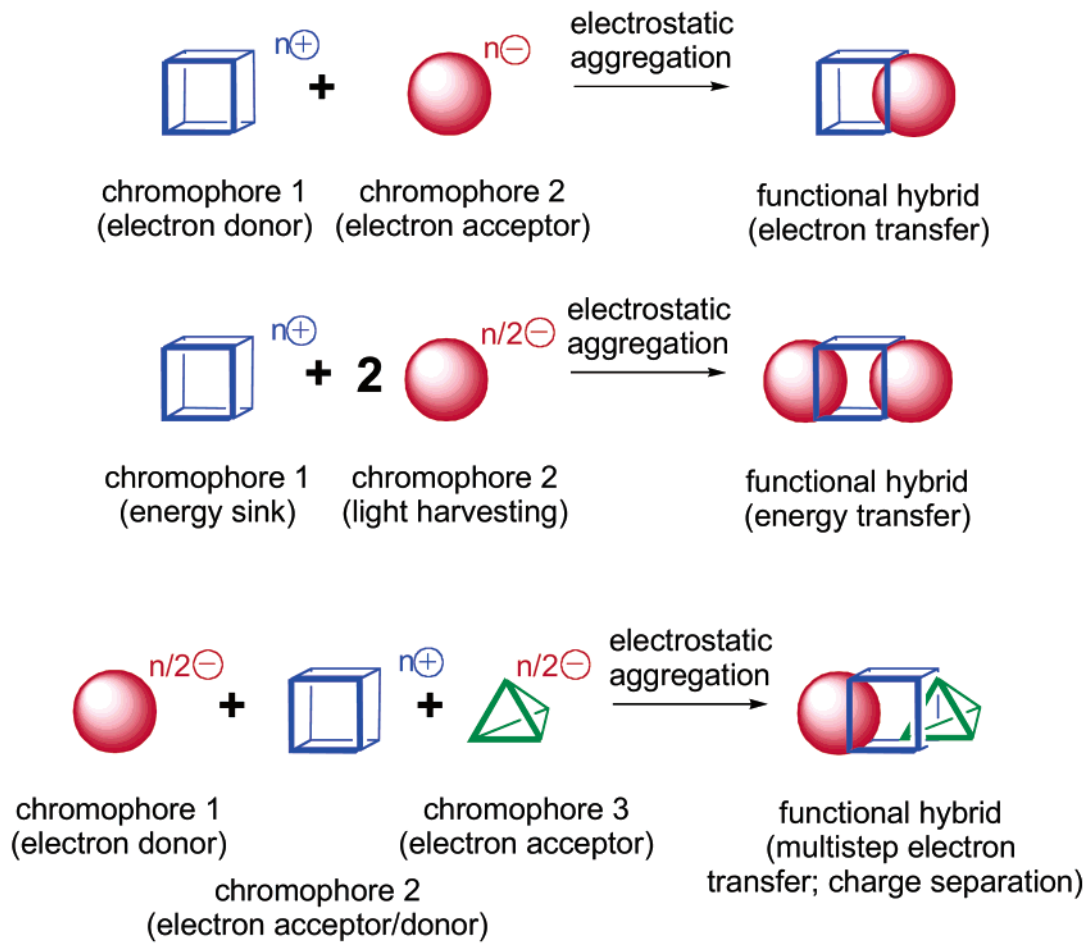

Figure 1. Schematic representation of discrete functional supramolecular assemblies consisting of different chromophores carrying matching charges (arbitrary assignment).

These so-obtained minimized structures were then subjected each to a MD calculation that started at 0 K with subsequent heating to 500 K for a time of 30 ps and kept at 500 K for another 20 ps. The MD simulations at 500 K of combined $\mathbf{1}^{8-}$ and $\mathbf{ZnP}^{8+}$ were started at a center-to-center distance between the porphyrin and the fullerene of approximately 45 Å but with 10 different orientations. Heating for 10 ps (0.5 fs step size) without force field cutoffs allowed the molecules to attract each other. Cooling the system to 0 K in 25 ps enabled the determination of minimum energies.

Results and Discussion

Compound **1** behaves as a typical fullerene monoadduct with UV/vis absorptions (H_2O, pH 7.2, phosphate buffer) at 254 nm (ϵ = 88 000 M^{-1} cm^{-1}), 322 nm (29 000 M^{-1} cm^{-1}), 424 nm (2500 M^{-1} cm^{-1}), and 466 nm (1700 M^{-1} cm^{-1}).[5] Although **1** is soluble in organic solvents, its octaanion $\mathbf{1}^{8-}$ is not. The porphyrin derivative $\mathbf{ZnP}^{8+}$ shows a significantly different electronic behavior when compared to other zinc porphyrins. In particular, the UV/vis absorptions show shifts around 14 nm for the Soret and 17 nm for the Q-band [H_2O, pH 7.2, phosphate buffer, 322 nm (ϵ = 407 000 M^{-1} cm^{-1}), 416 nm (102 000 M^{-1} cm^{-1}), 436 nm (429 000 M^{-1} cm^{-1}), 567 nm (21 200 M^{-1} cm^{-1}), and 606 (9300 M^{-1} cm^{-1})]. $\mathbf{ZnP}^{8+}$ is soluble in chlorinated hydrocarbons and methanol, as well as water, and shows solvochromic properties ($CHCl_3$, 321, 412, 433, 564, and 601 nm).[8] This indicates that $\mathbf{ZnP}^{8+}$ is susceptible to the formation of contact ion pairs with its bromide counterions in medium polar solvents, whereas in water solvent strictly separated ion pairs are present. In buffered aqueous solutions (pH 7.2, phosphate buffer), **1** and $\mathbf{ZnP}^{8+}$ are apparent as octaanion and octacation, respectively; that is, they have matching charges. Please note that when aqueous solutions of $\mathbf{1}^{8-}$ and $\mathbf{ZnP}^{8+}$ of concentrations higher than 10^{-3} M were mixed a precipitate, presumably a 1:1 complex, is formed. Therefore we performed our assays with concentrations for both electrolytes between 10^{-5} and 10^{-6} M, which limited our analysis to the spectral region of the porphyrin Soret band.

Upon addition of $\mathbf{1}^{8-}$ to $\mathbf{ZnP}^{8+}$, a 4 nm bathochromic shift of the $\mathbf{ZnP}^{8+}$ Soret band (i.e., from 436 to 440 nm) is discernible. This prompts a change of the electronic environment that the porphyrin chromophore experiences upon binding $\mathbf{1}^{8-}$. With this rather sensitive marker in hand, we applied the method of continuous variation of the concentrations with constant total concentration, Job plot, for several mixtures of $\mathbf{ZnP}^{8+}$ and $\mathbf{1}^{8-}$. Most importantly, both compounds form a stable 1:1 aggregate in aqueous buffered solution (pH = 7.2, ionic strength = 0.012). The absorptions were normalized using the procedure of Likussar,[13] which affords the normalized absorption versus molar fraction relationship in Figure 2. At the maximum, the curve reaches about 88% of the theoretical value, which can be transformed into an approximate association constant for $\mathbf{ZnP}^{8+}/\mathbf{1}^{8-}$ of (3.5 ± 1.0) × 10^8 M^{-1} (see Experimental Methods). This K_a value agrees well with that found for dimers formed by pairing anionic and cationic porphyrins analyzed by Linschitz.[15] Anionic porphyrins form complexes with **Cyt*c*** with association constants in the range of 2 × 10^6 [16] and 5 × 10^8 M^{-1}.[2,17] Similar association constants are also found

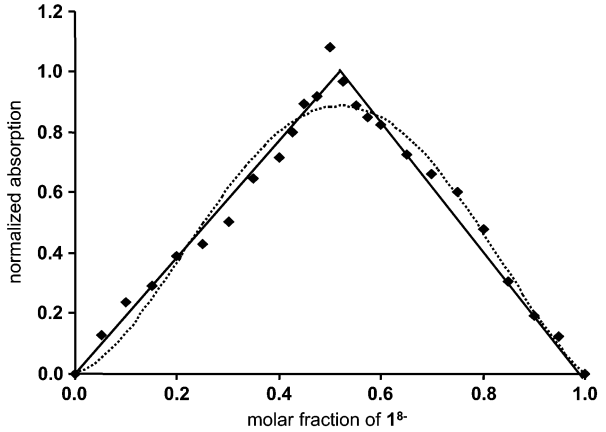

Figure 2. Job plot (Likussar modification) of molar fraction of $\mathbf{1}^{8-}$ versus normalized absorbance: (♦) actual data points; (—) linear fit on half set of data points; (···) fourth-power fit on all data points.

in the interaction of anionic and cationic cyclodextrins with up to eight charges on each compound.[18] We rule out that a 2:2 aggregate is formed because the Job plot does not show the intermediate 2:1 or 1:2 complexes being formed. Also, MD simulations (see below) indicate that about four to six of the porphyrin charges are paired with fullerene carboxylates. The remaining charges are compensated by the various ions in the buffer solution. With regard to the low concentrations of the components, the formation of higher aggregates seems even less likely.

On increase of the ionic strength of the solution, namely, addition of appropriate amounts of sodium bromide (ionic strength = 0.012 to 0.1), the $\mathbf{ZnP}^{8+}/\mathbf{1}^{8-}$ complex dissociates into the individual, free fragments, proving that the Coulomb force plays the dominant role in the association process. Very likely, direct π-stacking effects play no role because the fullerene core cannot get in close contact with the porphyrin or the pyridinium units.

We demonstrated above the importance of electrostatic interactions prevailing between the positively charged $\mathbf{ZnP}^{8+}$ and the negatively charged $\mathbf{1}^{8-}$ components for an evident trend toward the well-directed and oriented assembly of a 1:1 supramolecular $\mathbf{ZnP}^{8+}/\mathbf{1}^{8-}$ complex. The simple mixing of the individual components leads to a novel superstructure, for which one might expect that the highly fluorescent state of the singlet excited $\mathbf{ZnP}^{8+}$ state is quenched, for example, by an intracomplex electron transfer to the electron-accepting $\mathbf{1}^{8-}$.

In steady-state experiments, the $\mathbf{ZnP}^{8+}$ fluorescence (E_{singlet} = 2.02 eV) is characterized by maxima at 615 and 670 nm, see Figure 3 (top). Evidence for the electron-transfer deactivation stems from titration experiments of a 1.3×10^{-5} M solution of $\mathbf{ZnP}^{8+}$ with variable $\mathbf{1}^{8-}$ concentrations in the range between 0.28×10^{-5} and 3.0×10^{-5} M. Precisely upon excitation at 440 or 570 nm, the Soret and Q-band maxima of the $\mathbf{ZnP}^{8+}$ chromophore in the ground state, in aqueous solutions, a $\mathbf{1}^{8-}$ concentration-dependent decrease in intensity of the $\mathbf{ZnP}^{8+}$ fluorescence maxima is seen (Figure 4). At higher $\mathbf{1}^{8-}$ concentrations a plateau value is reached, at which the complexation of $\mathbf{ZnP}^{8+}$ is assumed to be complete and the effective concentration of $\mathbf{ZnP}^{8+}/\mathbf{1}^{8-}$ exceeds at least 95%. It should be noted that a purely diffusion-driven process can be ruled out on the basis of the applied $\mathbf{1}^{8-}$ concentrations and the short lifetime of the $\mathbf{ZnP}^{8+}$ singlet excited state (vide supra). A closer inspection of Figure 3 (top) reveals that simultaneous with the quenched $\mathbf{ZnP}^{8+}$ fluorescence at 615 and 670 nm, the fluorescence spectra are subject to a small red shift (i.e., ca. 2 nm).

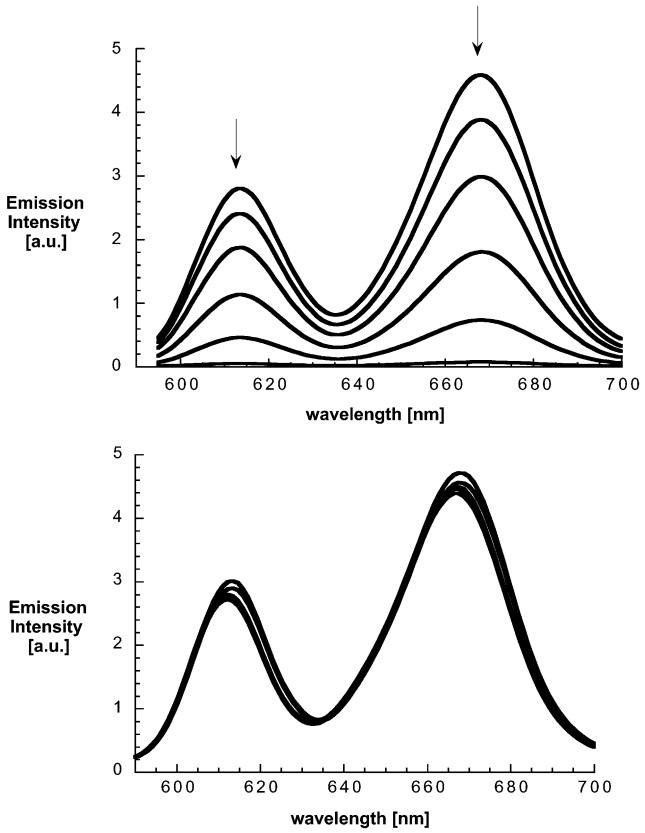

Figure 3. Steady-state fluorescence spectra (λ_{exc} = 420 nm) of $\mathbf{ZnP}^{8+}$ (1.3×10^{-5} M) and variable concentration of (top) $\mathbf{1}^{8-}$ (0.28×10^{-5} M, 0.57×10^{-5} M, 0.85×10^{-5} M, 1.13×10^{-5} M, 1.42×10^{-5} M, and 2.1×10^{-5} M) and (bottom) × reference dendron ($(0.28-3.0) \times 10^{-5}$ M) in H_2O at room temperature, pH 7.2, 0.05 M Na_2HPO_4.

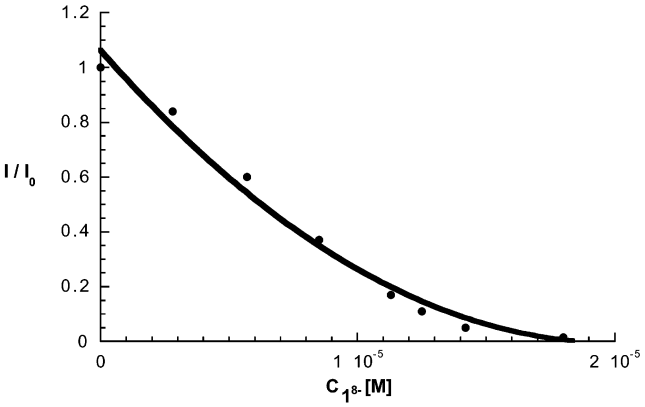

Figure 4. I/I_0 of $\mathbf{ZnP}^{8+}$ versus concentration of $\mathbf{1}^{8-}$ relationship used to determine the association constant. The fitted curve gives a χ^2 value of 1.011.

This tracks the shift seen in the $\mathbf{ZnP}^{8+}$ ground-state spectrum upon association with $\mathbf{1}^{8-}$. On the other hand, direct evidence for emissive charge-transfer features, as seen earlier for covalently linked $ZnP-C_{60}$ dyads, were not concluded.[19] Titration experiments with 1.3×10^{-5} M solution of $\mathbf{ZnP}^{8+}$ and variable concentrations (i.e., between 0.25×10^{-5} and 3.5×10^{-5} M) of the dendrimer system $\mathbf{2}^{8-}$ lacking the fullerene core led to no significant fluorescence quenching, see Figure 3 (bottom).

Prior to the addition of $\mathbf{1}^{8-}$, the fluorescent signal of $\mathbf{ZnP}^{8+}$ is well fitted by a monoexponential decay, for which a lifetime of 2.5 ns was determined in deoxygenated pH 7.2 solutions. This lifetime is in good agreement with previously published values for zinc tetraphenylporphyrins in various media.[20] After

TABLE 1: Association Constants and Fluorescence Lifetimes of $ZnP^{8+}/1^{8-}$ under Different Experimental Conditions

conditions	pH	K [M^{-1}]	fluorescence lifetime (τ) $ZnP^{8+}/1^{8-}$ (ns)
deionized water	7.2	1.1×10^8	2.5/0.12
0.005 N Na phosphate buffer[a]	7.2	2.8×10^7	
0.005 N Na phosphate buffer[a]	8.4	1.1×10^8	
0.05 N Na phosphate buffer[a]	7.2	9.5×10^6	2.3/0.11
0.1 N $NaCHO_2$[b]	7.2	4.6×10^6	
0.1 N NaF[b]	7.2	2.7×10^7	2.5/0.09
0.1 N NaCl[b]	7.2	2.2×10^6	
0.1 N NaBr[b]	7.2	3.5×10^6	

[a] Purchased from Aldrich, containing NaH_2PO_4 and NaOH. [b] Buffered with 5 mM sodium phosphate buffer.

the addition of $\mathbf{1}^{8-}$, the fluorescent signal of $\mathbf{ZnP}^{8+}$ exhibits a double-exponential decay with lifetimes of 2.5 and 0.12 ns. The two lifetimes are maintained throughout the titration assay with, however, relative increase and decrease in weight of the short-lived and long-lived components, respectively, on increase of the concentrations of $\mathbf{1}^{8-}$. Ultimately, the plateau region is reached, where only the short-lived component is monitored. Addition of acid restores the original $\mathbf{ZnP}^{8+}$ fluorescence intensity, concomitant with the disappearance of the short-lived component and the reappearance of the long-lived component.

On the basis of the aforementioned results, we reach the following conclusion. The decrease of fluorescence intensity in $\mathbf{ZnP}^{8+}$, the shift of the $\mathbf{ZnP}^{8+}$ fluorescence, and evidence for a short-lived emissive component, which renders invariant throughout the titration assay, all realized upon addition of $\mathbf{1}^{8-}$, suggest a static quenching event inside a well-defined supramolecular $\mathbf{ZnP}^{8+}/\mathbf{1}^{8-}$ complex. In the $\mathbf{ZnP}^{8+}/\mathbf{1}^{8-}$ complex, the fluorescent state of $\mathbf{ZnP}^{8+}$, which is a good electron donor, is quenched by charge transfer to the electron-accepting $\mathbf{1}^{8-}$ and, accordingly, substituted by a long-lived charge-separated state, see below.

Fitting the I/I_0 versus $\mathbf{1}^{8-}$ titration curve to the procedure[21]

$$I = I_0 + \frac{\Delta I}{2S_0}[K_{diss} + X + S_0 - \sqrt{(K_{diss} + X + S_0)^2 - 4XS_0}]$$

we obtain a value of $(1.1 \pm 0.1) \times 10^8$ M^{-1} for the association constant of the supramolecular $\mathbf{ZnP}^{8+}/\mathbf{1}^{8-}$ complex at pH 7.2. I, I_0, and ΔI ($\Delta I = I_0 - I$) are the fluorescence intensities observed at 613 nm, $K_{diss} = 1/K_{assoc}$, and X and S_0 are the titrant ($\mathbf{1}^{8-}$) and substrate ($\mathbf{ZnP}^{8+}$) concentrations, respectively. To probe the influence of ionic strength on the $\mathbf{ZnP}^{8+}/\mathbf{1}^{8-}$ association, we carried out analogous $\mathbf{ZnP}^{8+}$ versus $\mathbf{1}^{8-}$ titration experiments in the presence of different salts, at different concentration, and at different pH. Table 1 tabulates the correspondingly determined K-values. Depending on the effective ionic strength and the size of the anion, the association constants were as low as 2.2×10^6 M^{-1}, for the case of 0.1 N NaCl. Interestingly, at 0.05 N Na_2HPO_4, that is, at the same ionic strength, the constant is nearly 4-times larger. In other words, the smaller Cl-anions, relative to the HPO_4-dianions, evoke weaker bindings. Similar trends were also observed for the larger HCO_2- and Br-anions. Similarly, Schneider et al. noted that the association constant of Coulomb complexes of, for example, several tetracationic porphyrins and anionic nucleotides varies by at least 2 numbers of magnitudes depending on the buffer concentrations.[22] No effects, on the other hand, were seen for the fluorescence lifetimes. When the pH of the buffer solution was raised from 7.2 to 8.4, a significant increase of the binding constant was observed. As was stated earlier, at pH 7.2, the predominant species is $\mathbf{1}^{8-}$; nevertheless, other ionic species, such as $\mathbf{1}^{9-}$, $\mathbf{1}^{7-}$, or $\mathbf{1}^{6-}$, are present in the mixture via protonation/deprotonation equilibria. The higher pH obviously shifts these equilibria toward a higher effective concentration of $\mathbf{1}^{8-}$ and $\mathbf{1}^{9-}$.

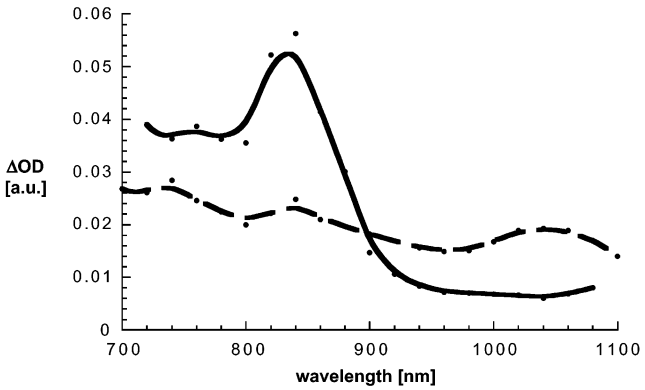

Figure 5. Transient absorption spectrum (NIR part) of $\mathbf{ZnP}^{8+}$ (1.0×10^{-5} M) in the absence (—) and presence of $\mathbf{1}^{8-}$ (ca. 1.0×10^{-5} M) (— — —) recorded 50 ns following an 8 ns laser pulse ($\lambda_{exc} = 532$ nm) showing the characteristic $C_{60}^{\bullet-}$ fingerprint with λ_{max} at 1040 nm.

To confirm the electron-transfer quenching of $\mathbf{ZnP}^{8+}$, transient absorption spectroscopy, following 8 ns laser excitation at 532 nm, was performed with $\mathbf{ZnP}^{8+}$ in the absence and presence of $\mathbf{1}^{8-}$. In the absence of $\mathbf{1}^{8-}$, differential absorption spectra, recorded ca. 50 ns after the short laser pulse for a deoxygenated aqueous solution of $\mathbf{ZnP}^{8+}$ (1.0×10^{-5} M), are characterized by strong bleaching of the porphyrin's Q-band absorption at 570 nm (not shown). Further in the red, an instantaneous formation of broad absorptions at wavelengths >600 nm including a distinct maximum at 840 nm is discernible, see Figure 5. These spectral features are attributes of the long-lived $\mathbf{ZnP}^{8+}$ triplet excited state ($E_{triplet} = 1.53$ eV).[23] The picture associated with the nanosecond absorption spectroscopy in the presence of $\mathbf{1}^{8-}$ (ca. 10^{-5} M) is different. Despite the unequivocal excitation of $\mathbf{ZnP}^{8+}$ at 532 nm (i.e., absorption ratio $\mathbf{ZnP}^{8+}$ versus $\mathbf{1}^{8-} = 4/1$), no porphyrin triplet−triplet absorption was found at short delay times following the 8 ns laser pulse in oxygen-free solutions. Instead, a new transient develops as a result of the rapid intracomplex deactivation of the $\mathbf{ZnP}^{8+}$ excited state. A key feature of the new products is a broad maximum in the visible region around 650 nm, which resembles the well-known one-electron oxidized parent zinc tetraphenylporphyrin (**ZnTPP**) π-radical cation, $\mathbf{ZnTPP}^{\bullet+}$.[24] Concomitant with the $(\mathbf{ZnP}^{8+})^{\bullet+}$ features in the visible, we noticed a near-infrared maximum at 1040 nm, corroborating the one-electron reduction of the electron-accepting fullerene, $(\mathbf{1}^{8-})^{\bullet-}$.[25] Due to the large spatial separation, the $(\mathbf{ZnP}^{8+})^{\bullet+}/(\mathbf{1}^{8-})^{\bullet-}$ decays rather slowly, from which we derive a lifetime of 1.1 μs. The charge recombination process is dominated by a monoexponential recovery of the singlet ground state rather than population of a porphyrin triplet excited state. This observation corresponds well with the energetic argument (~1.35 eV).

Calculations

To gain further insight into the structure of the $\mathbf{ZnP}^{8+}/\mathbf{1}^{8-}$ complex, we first PM3-optimized the octapyridinium zinc porphyrin salt $\mathbf{ZnP}^{8+}$ and the dendritic fullerene oligocarboxylate $\mathbf{1}^{8-}$, both in the absence of counterions. Implicit is in this picture that the 1:1 complex $\mathbf{ZnP}^{8+}/\mathbf{1}^{8-}$ assumes a neutral configuration. After MD-simulated heating to 500 K in 30 ps and a period of

20 ps at this temperarure, $\mathbf{ZnP}^{8+}$ showed several conformations with two noteworthy extremes: first, a double-cone-shaped conformation with the pyridinium units pointing to the outside of the molecule and, second, a π-stacked conformation in which two diametrically opposed pyridinium units sit right atop the center of the porphyrin. The latter is, according to PM3 calculations at 0 K, more stable than the cone-shaped conformation. The electrostatic repulsion, potentially existing between pyridinium moieties, seems weak, which can be understood on the basis of mesomeric charge distribution in these groups. In contrast, performing a similar MD simulation with $\mathbf{1}^{8-}$, we observe a dendrimer structure with widely extended branches.

Then 10 separate and independent MD calculations at 500 K were performed with the aforementioned double-cone-shaped $\mathbf{ZnP}^{8+}$ and $\mathbf{1}^{8-}$, both compounds being heated to 500 K (see above), in which both compounds were placed at center-to-center distances of approximately 45 Å but with various orientations toward each other. During a period of 10 ps, the molecules were allowed to attract each other, which led to a rather fast formation of $\mathbf{ZnP}^{8+}/\mathbf{1}^{8-}$, and then they were cooled in 25 ps to 0 K. Although the small size of both molecules prohibited any apparent selectivity, some topological traits were observed. In particular, as soon as one salt bridge is formed, the other bridges were quickly built leading to a structure in which $\mathbf{1}^{8-}$ covers about one-half of $\mathbf{ZnP}^{8+}$ (Figure 6). Roughly, four to six of the pyridinium units build salt bridges with the carboxylate anions of $\mathbf{1}^{8-}$. In addition, a bending of the "free" pyridinium units toward the carboxylates of $\mathbf{1}^{8-}$ was found. This topological feature is observed in basically all calculations with energies varying in a range of approximately 10%. This indicates that even in an electrostatically saturated complex strong attracting forces are still effective. An averaged distance of 8 Å between the π-surfaces of the two chromophores is deduced from the minimized complexes. The major limitation of these calculations carried out in the gas phase is the irreversible formation of the electrostatic interactions between $\mathbf{ZnP}^{8+}$ and $\mathbf{1}^{8-}$. Simulations of the complexes in a periodic water box are currently under way.

Conclusion and Outlook

$\mathbf{ZnP}^{8+}$ and $\mathbf{1}^{8-}$ form a very strong supramolecular complex in which intracomplex electron transfer takes place to generate a charge-separated species $(\mathbf{ZnP}^{8+})^{\bullet+}/(\mathbf{1}^{8-})^{\bullet-}$, which decays with a remarkably long lifetime of 1.1 μs. Stability investigations showed the expected disassembly of the complex at higher ionic strength with little dependence on the nature of the anions. Coulomb interactions play obviously the major role in the aggregation process. The topological parameters of the $\mathbf{ZnP}^{8+}/\mathbf{1}^{8-}$ complex were calculated by MD simulations, which give a $\pi-\pi$ distance of about 8 Å. Interestingly, $\mathbf{1}^{8-}$ is not able to cover $\mathbf{ZnP}^{8+}$ completely but leaves approximately half of the molecule exposed. It seems reasonable to assume that if a chromophore with more than a single dendritic polyanionic entity would have been taken, instead of $\mathbf{1}^{8-}$, much larger aggregates will be formed that may consist, for example, of linear $[\mathbf{ZnP}^{8+}/\mathbf{chromophore}^{m-}]_n$ chains with an accumulation of negative charges due to the excess of carboxylates. In principle, other anionic polyelectrolytes could be electrostatically attached to the free half of the porphyrin. Also, replacing the non-redox-active zinc ion with, for example, Co^{2+} or Ru^{2+} could lead to interesting supramolecular redox-active Coulomb complexes. Axial coordination to the porphyrin metal could allow for even more intricate structures. It is noteworthy to mention that the fullerene module **1** is also easily modified by variation of the dendritic parts or by addition of further substituents to the fullerene core. These variations can be further extended to more complex constructs when the electrostatic aggregation process is controlled via layer-by-layer formation on a surface.[6,26]

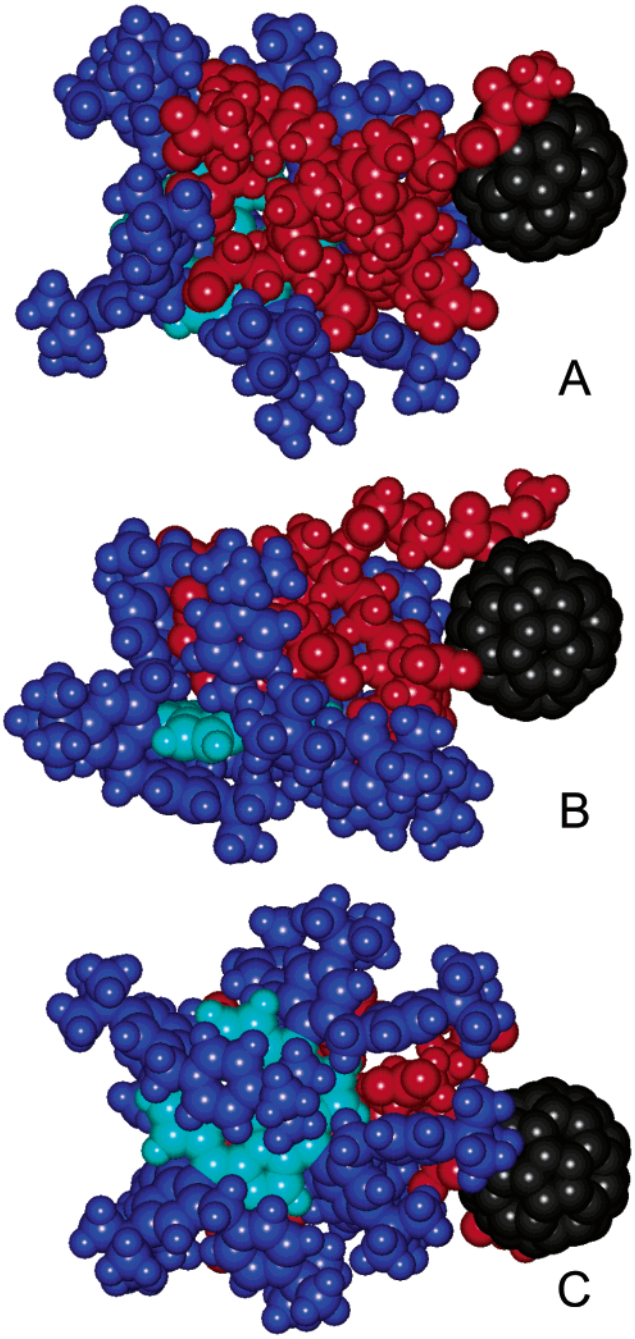

Figure 6. Typical MD simulated model of the $\mathbf{ZnP}^{8+}/\mathbf{1}^{8-}$ complex: (black) fullerene residue of $\mathbf{1}^{8-}$; (red) dendrimer part of $\mathbf{1}^{8-}$ with eight carboxylates; (cyan) zinc porphyrin chromophore of $\mathbf{ZnP}^{8+}$; (blue) phenyl rings of $\mathbf{ZnP}^{8+}$ with eight pyridinium units; (A) top view; (B) side view; (C) bottom view.

Acknowledgment. We thank the Deutsche Forschungsgemeinschaft (Grant SFB 583 Redoxaktive Metallkomplexe − Reaktivitätssteuerung durch molekulare Architekturen) for financial support. N.J. thanks the DFG for a scholarship. Part of this work was supported by the Office of Basic Energy Sciences of the U.S. Department of Energy. This is document NDRL 4488 from the Notre Dame Radiation Laboratory.

References and Notes

(1) (a) Isied, S. S.; Worosila, G.; Artherton, S. J. *J. Am. Chem. Soc.* **1982**, *104*, 7659−7661. (b) Isied, S. S. *Adv. Chem. Ser.* **1997**, *253*, 331−347. (c) McArdle, J. V.; Gray, H. B.; Creutz, C.; Sutin, N. *J. Am. Chem. Soc.* **1974**, *96*, 5737−5741. (d) McArdle, J. V.; Yocom, K.; Gray, H. B. *J. Am. Chem. Soc.* **1977**, *12*, 4141−4145. (e) Meier, M.; van Eldik, R. *Inorg. Chim. Acta* **1994**, *225*, 95−101. (f) Meier, M.; van Eldik, R.; Chang, I. J.; Mines, G. A.; Wuttke, D. S.; Winkler, J. R.; Gray, H. B. *J. Am. Chem. Soc.* **1994**, *116*, 1577−1578. (g) Meier, M.; Sun, J.; van Eldik, R.; Wishart, J. F. *Inorg. Chem.* **1996**, *35*, 1564−1570. (h) Meier, M.; van Eldik, R. *Inorg. Chim. Acta* **1996**, *242*, 185−189. (i) Meier, M.; van Eldik, R. *Chem.−Eur. J.* **1997**, *3*, 39−46.

(2) Jain, R. K.; Hamilton, A. D. *Angew. Chem., Int. Ed.* **2002**, *41*, 641−643.

(3) (a) Decher, G. *Science* **1997**, *277*, 1232−1237. (b) Kaschak, D. M.; Lean, J.-T.; Waraksa, C. C.; Saupe, G. B.; Usami, H.; Mallouk, T. E. *J. Am. Chem. Soc.* **1999**, *121*, 3435−3445.

(4) (a) Hirsch, A. *The Chemistry of the Fullerenes*; Georg Thieme Verlag: Stuttgart, Germany, New York, 1994. (b) Hirsch, A. *Top. Curr. Chem.* **1999**, *199*, 1−65.

(5) Braun, M.; Atalick, S.; Guldi, D. M.; Lanig, H.; Brettreich, M.; Burghardt, S.; Hatzimarinaki, M.; Ravanelli, E.; Prato, M.; van Eldik, R.; Hirsch, A. *Chem.−Eur. J.* **2003**, *9*, 3867−3875.

(6) For polyelectrolyte layer-by-layer assemblies, see: (a) Decher, G.; Hong, J. D. *Ber. Bunsen-Ges. Phys. Chem.* **1991**, *95*, 1430−1434. (b) Decher, G.; Eckle, M.; Schmitt, J.; Struth, B. *Curr. Opin. Colloid Interface Sci.* **1998**, *3*, 32−39. (c) Arys, X.; Jonas, A. M.; Laschewsky, A.; Legras, R. In *Supramolecular Polymers*; Cifferi, A., Ed.; Marcel Dekker: New York, 2000; p 505. (d) Bertrand, P.; Jonas, A. M.; Laschewsky, A.; Legras, R. *Macromol. Rapid Commun.* **2000**, *21*, 319−348. (e) Arys, X.; Fischer P.; Jonas, A. M.; Koetse, M. M.; Laschewsky, A.; Legras, R.; Wischerhoff, E. *J. Am. Chem. Soc.* **2003**, *125*, 1859−1865.

(7) (a) Ruhlmann, L.; Zimmermann, J.; Fudickar, W.; Siggel, U.; Fuhrhop, J.-H. *J. Electroanal. Chem.* **2001**, *503*, 1−14. (b) Li, G.; Fudickar, W.; Skupin, M.; Klyszcz, A.; Draeger, C.; Lauer, M.; Fuhrhop, J.-H. *Angew. Chem., Int. Ed.* **2002**, *41*, 1828−1852. (c) Fudickar, W.; Zimmermann, J.; Ruhlmann, L.; Schneider, J.; Roeder, B.; Siggel, U.; Fuhrhop, J.-H. *J. Am. Chem. Soc.* **1999**, *121*, 9539−9545.

(8) Jux, N. *Org. Lett.* **2000**, *2*, 2129−2132.

(9) Holten, D.; Bocian, D. F.; Lindsey, J. S. *Acc. Chem. Res.* **2002**, *35*, 57−69.

(10) (a) Vicente, M. G. H. In *The Porphyrin Handbook, Vol. 1, Synthesis and Organic Chemistry*; Kadish, K. M., Smith, K. M., Guilard, R., Eds.; Academic Press: San Diego, CA, 2000; pp 149−199. (b) Jaquinod, L. In *The Porphyrin Handbook, Vol. 1, Synthesis and Organic Chemistry*; Kadish, K. M., Smith, K. M., Guilard, R., Eds.; Academic Press: San Diego, CA, 2000, pp 201−237. (c) Sanders, J. K. M.; Bampos, N.; Clyde-Watson, Z.; Darling, S. L.; Hawley, J. C.; Kim, H.-J.; Mak, C. C.; Webb, S. J. In *The Porphyrin Handbook, Vol. 3, Inorganic, Organometallic and Coordination Chemistry*; Kadish, K. M., Smith, K. M., Guilard, R., Eds.; Academic Press: San Diego, CA, 2000, pp 1−40.

(11) (a) Croke, D. T.; Perrouault, L.; Sari, M. A.; Battioni, J. P.; Mansuy, D.; Helene, C.; Trung Le, D. *J. Photochem. Photobiol., B* **1993**, *18*, 41−50. (b) Sari, M. A.; Battioni, J. P.; Dupre, D.; Mansuy, D.; Le Pecq, J. B. *Biochemistry* **1990**, *29*, 4205−4215. (c) Lipscomb, L. A.; Zhou, F. X.; Presnell, S. R.; Woo, R. J.; Peek, M. E.; Plaskon, R. R.; Williams, L. D. *Biochemistry* **1996**, *35*, 2818−2823. (d) Arthanari, H.; Bolton, P. H. *Anti-Cancer Drug Des.* **1999**, *14*, 317−326. Izbicka, E.; Wheelhouse, R. T.; Raymond, E.; Davidson, K. K.; Lawrence, R. A.; Sun, D.; Windle, B. E.; Hurley, L. H.; Von Hoff, D. D. *Cancer Res.* **1999**, *59*, 639−644. (e) Shi, D. F.; Wheelhouse, R. T.; Sun, D.; Hurley, L. H. *J. Med. Chem.* **2001**, *44*, 4509−4523. (f) Patel, M.; Day, B. J. *Trends Pharmacol. Sci.* **1999**, *20*, 359−364. (g) DeCamp, D. L.; Babe, L. M.; Salto, R.; Lucich, J. L.; Koo, M. S.; Kahl, S. B.; Craik, C. S. *J. Med. Chem.* **1992**, *35*, 3426−3428.

(12) For a notable exception, see: Almarsson, Ö.; Adalsteinsson, H.; Bruice, T. C. *J. Am. Chem. Soc.* **1995**, *117*, 4524−4532.

(13) Likussar, W.; Boltz, D. F. *Anal. Chem.* **1971**, *43*, 1265−1272.

(14) *HyperChem 6.03 and 7.0*, evaluation release; HyperCube, Inc.: Gainesville, FL, 2002.

(15) (a) Ojadi, E.; Selzer, R.; Linschitz, H. *J. Am. Chem. Soc.* **1985**, *107*, 7783−7784. (b) van Willigen, H.; Das, U.; Ojadi, E.; Linschitz, H. *J. Am. Chem. Soc.* **1985**, *107*, 7784−7785.

(16) Clark-Ferris, K. K.; Fisher, J. *J. Am. Chem. Soc.* **1985**, *107*, 5007−5008.

(17) Jain, K. R.; Hamilton, A. D. *Org. Lett.* **2000**, *2*, 1721−1723.

(18) (a) Hamelin, B.; Jullien, L.; Derouet, C.; du Penhoat, C. H.; Berthault, P. *J. Am. Chem. Soc.* **1998**, *120*, 8438−8447. (b) Jullien, L.; Cottet, H.; Hamelin, B.; Jardy, A. *J. Phys. Chem. B* **1999**, *103*, 10866−10875.

(19) (a) Armaroli, N.; Marconi, G.; Echegoyen, L.; Bourgeois, J.-P.; Diederich, F. *Chem.−Eur. J.* **2000**, *6*, 1629−1645. (b) Imahori, H.; Tkachenko, N. V.; Vehmanen, V.; Tamaki, K.; Lemmetyinen, H.; Sakata Y.; Fukuzumi, S. *J. Phys. Chem. A* **2001**, *105*, 1750−1756. (c) Guldi, D. M.; Luo, C.; Prato, M.; Troisi, A.; Zerbetto, F.; Scheloske, M.; Dietel, E.; Bauer, W.; Hirsch, A. *J. Am. Chem. Soc.* **2001**, *123*, 9166−9167.

(20) (a) Murov, S. L.; Carmichael, I.; Hug, G. L. *Handbook of Photochemistry*; Marcel Dekker Inc.: New York, 1993. (b) Hoffman, M. Z.; Bolletta, F.; Moggi, L.; Hug, G. L. *J. Phys. Chem. Ref. Data* **1989**, *18*, 219.

(21) (a) Famigni, L.; Johnston, M. B. *New. J. Chem.* **2001**, *25*, 1368−1370. (b) Encinas, S.; Bushell, K. L.; Couchman, S. M.; Jeffery, J. C.; Ward, M. D.; Flamigni, L.; Barigelletti, F. *J. Chem. Soc., Dalton Trans.* **2000**, 1783−1792.

(22) Sirish, M.; Schneider, H.-J. *Chem. Commun.* **2000**, 23−24.

(23) Rodriguez, J.; Kirmaier, C.; Holten, D. *J. Am. Chem. Soc.* **1989**, *111*, 6500−6506.

(24) (a) Luo, C.; Guldi, D. M.; Imahori, H.; Tamaki, K.; Sakata, Y. *J. Am. Chem. Soc.* **2000**, *122*, 6535−6551. (b) Imahori, H.; Tamaki, K.; Guldi, D. M.; Luo, C.; Fujitsuka, M.; Ito, O.; Sakata, Y.; Fukuzumi, S. *J. Am. Chem. Soc.* **2001**, *123*, 2607−2617. (c) Fukuzumi, S.; Imahori, H.; Yamada, H.; El-Khouly, M. E.; Fujitsuka, M.; Ito, O.; Guldi, D. M. *J. Am. Chem. Soc.* **2001**, *123*, 2571−2575.

(25) Guldi, D. M.; Prato, M. *Acc. Chem. Res.* **2000**, *33*, 695−703.

(26) Guldi, D. M.; Martin, N. *J. Mater. Chem.* **2002**, *12*, 1978−1992.